ELSEVIER

Journal of Molecular Catalysis A: Chemical 155 (2000) 59–71

JOURNAL OF MOLECULAR CATALYSIS A: CHEMICAL

www.elsevier.com/locate/molcata

Synergy between α-Sb_2O_4 and $Fe_2(MoO_4)_3$ during the first hours of the catalytic oxidation of isobutene to methacrolein

Yan-Liang Xiong [1], Lu-Tao Weng, Patrick Bertrand [2], Jean Ladrière [3], Loreto Daza [4], Patricio Ruiz, Bernard Delmon *

Unité de Catalyse et Chimie des Matériaux Divisés, Université Catholique de Louvain, Place Croix du Sud 2 / 17, 1348 Louvain-la-Neuve, Belgium

Received 6 January 1999; accepted 16 April 1999

Abstract

The physico-chemical properties and the catalytic behaviour of mixtures of iron molybdate and antimony oxide in the selective oxidation of isobutene to methacrolein were studied with special consideration of the possibility of changes of these oxides during the catalytic reaction. The catalysts were separately prepared $Fe_2(MoO_4)_3$ and α-Sb_2O_4 and mixtures thereof. They were characterized by BET surface area measurements, X-ray diffraction (XRD), Conventional Transmission Electron Microscopy (CTEM), Electron Probe Micro Analysis (EPMA), X-ray Photoelectron Spectroscopy (XPS), Ion Scattering Spectroscopy (ISS) and Mössbauer spectroscopy before and after the catalytic reaction. Under the reaction conditions used, no mutual contamination was detectable neither before nor after test. Pure α-Sb_2O_4 is inactive. $Fe_2(MoO_4)_3$ is active but poorly selective. The α-Sb_2O_4–$Fe_2(MoO_4)_3$ mixtures exhibit a synergetic effect, corresponding to an increase both in the methacrolein yield and in the selectivity to methacrolein. The donor properties of α-Sb_2O_4 and the acceptor properties of the $Fe_2(MoO_4)_3$ oxide can explain this synergism in the frame of the Remote Control theory: oxygen spillover would be emitted by α-Sb_2O_4, and migrate to $Fe_2(MoO_4)_3$, creating or regenerating selective sites on this last phase. The beneficial effect of spillover oxygen seems to reside in its ability to keep iron in a higher oxidation state, close to Fe^{+3}.

Keywords: Catalytic synergy; Oxide catalysts; Isobutene oxidation

1. Introduction

The elemental composition of almost all active and selective oxidation catalysts is very complex, and it is now well established that they contain several phases which work synergetically. Among the different theories proposed to explain synergy, the remote control mecha-

* Corresponding author. Tel.: +32-10-473590; fax: +32-10-473649; e-mail: delmon@cata.ucl.ac.be

[1] On leave from the Chemistry Department, Xiamen University, Xiamen, China.

[2] Unité de Physico-Chimie et de Physique des Matériaux, Université Catholique de Louvain, Louvain-la-Neuve, Belgium.

[3] Unité de Chimie Inorganique et Nucléaire, Université Catholique de Louvain, Louvain-la-Neuve, Belgium.

[4] On leave from the Instituto de Catalisis y Petroleoquimica, CSIC, Madrid, Spain.

1381-1169/00/$ - see front matter
PII: S1381-1169(99)00319-2

nism (RCM) seems adequate to explain many experimental results concerning multiphase catalysts. The explanation is that the synergetic effects are due to a long distance action exerted by one phase on the other. More precisely, some oxide phases (donors) are able to activate molecular oxygen and form a mobile species (spillover oxygen) which migrates to the other oxide phase (acceptor) to react with its surface and create or regenerate the sites which form selectively the partially oxygenated products [1–14].

The RCM is supported by studies dealing with reactions in which oxygen plays an important role: oxidation of isobutene to methacrolein [1,2,5–7,12,13], oxidation of butane to maleic anhydride [9], oxidative dehydrogenation of methanol to formaldehyde, ethanol to acetaldehyde [1,13], ethanol to acetic acid, butene to butadiene, propane or pentane to the corresponding olefins and the dehydration of formamides to nitriles in the presence of oxygen [3,4,14,19,20], etc. Experiments with ^{18}O, confirmed by FTIR and Raman spectroscopies, prove the occurrence of spillover processes in conditions where the RCM operates [8,15–17].

Very strong indications have been obtained showing that RCM modifies the coordination of surface catalytic atoms: formation of OH groups (Brönsted acids) on acceptors [1,2,4,9,19], inhibition in the formation of coke precursors [8], stabilization of surfaces at a more oxidized level with a parallel diminution of the amount of ''shear structures'' and reconstruction of surfaces [1,2,13,18]. The RCM also modifies the critical oxygen pressure leading to the deactivation of copper in the oxidative dehydrogenation of isopropanol [21].

Iron molybdate is an important component in many catalysts used in the oxidation or ammoxidation of propene to acrolein or acrylonitrile, respectively, and in the oxidation of methanol to formaldehyde. On the other hand, antimony oxide plays an important role in many other oxidation catalysts such as the Sn–Sb, Fe–Sb and U–Sb oxide systems.

The objective of the present paper is to better understand the mechanism underlying the cooperation between iron molybdate $Fe_2(MoO_4)_3$ and antimony oxide α-Sb_2O_4. Our objective is to study the possibility of existence of a RCM on this system. However, caution has to be taken because of the possibility that a mechanical mixture of two phases can get transformed into a different multiphasic catalyst during the reaction. New phases can be formed, the catalyst texture can also be modified, and consequently, several other processes may, in principle, explain the synergy. Actually, we had shown previously that calcination of $Fe_2(MoO_4)_3 + \alpha$-Sb_2O_4 mixtures at high temperature (600°C) promotes a solid state reaction forming new phases (MoO_3, $FeSbO_4$).

The present paper focuses on the phenomena occurring on fresh mixtures of α-Sb_2O_4 and $Fe_2(MoO_4)_3$, where no or little contamination has taken place. Our particular objective was to investigate whether a synergy exists before the starting oxides have substantially reacted with each other. We started from a suspension of the oxides evaporated under agitation. This method was chosen in order to minimize the chemical interaction between the two oxides. In mechanical mixtures, the role played by each phase can be identified more easily. The oxidation of isobutene to methacrolein was used to measure the catalytic activity of samples. The problem was to distinguish between several situations that may occur during the preparation of the mixture or the catalytic test. The phases may maintain their identity without any modification. But the formation of a new mixed phase such as $Fe_2Sb_2O_7$, $FeSbO_4$ or $FeMoO_4$ or mutual surface contamination in $Fe_2(MoO_4)_3$–α-Sb_2O_4 mechanical mixture may also occur.

All catalysts were characterized before and after reaction. X-ray diffraction (XRD) and Mössbauer spectroscopy techniques were used to detect changes and particularly the possible formation of a new phase or solid solution, or in the valency of Fe. Conventional Transmission Electron Microscopy (CTEM) and BET surface

area analysis were used to provide information about morphology, texture and size of catalyst particles, and their changes. The composition of individual particles was studied by Electron Probe Micro Analysis (EPMA). Two techniques were used to detect surface composition changes: X-ray Photoelectron Spectroscopy (XPS) and Ion Scattering Spectroscopy (ISS).

2. Experimental

2.1. Catalyst preparation

In all cases, pure grade liquid or solid reagents were used without any further purification.

2.1.1. Pure oxide phases

(a) Preparation of $Fe_2(MoO_4)_3$: 50 ml of an aqueous solution containing 17 ml of ethylenediamine (EN) (Merck, pure grade) acidified by nitric acid (pH = 0.5) were added to 100 ml of an aqueous solution containing 13.66 g of $Fe(NO_3)_3 \cdot 9H_2O$ (Merck, pure grade) ($C_{EN}/C_{Fe^{3+}} = 4/1$). The pH value of the mixed solution was adjusted to 1.0–1.5 by addition of pure ethylenediamine. This solution was mixed with 100 ml of an aqueous solution containing 8.95 g of $(NH_4)_6Mo_7O_{24} \cdot 4H_2O$ (Merck, pure grade) under stirring at 50°C. The solution was then evaporated in a Rotavapor and dried at 110°C. Finally, the dried powder was calcined at 500°C for 20 h. Yellowish monoclinic $Fe_2(MoO_4)_3$ with surface area of 2.5 $m^2\ g^{-1}$ was obtained.

(b) Preparation of α-Sb_2O_4: Sb_2O_3 (powder, Merck, pure grade) was calcined at 500°C for 20 h, then finely ground. White orthorhombic α-Sb_2O_4 with a surface area of 2.6 $m^2\ g^{-1}$ was obtained.

2.1.2. Preparation of mechanical mixtures of pure oxides

The mechanical mixtures of $Fe_2(MoO_4)_3$ and α-Sb_2O_4 were prepared by dispersing the two powders in *n*-pentane (Merck, pure grade) under alternatively magnetic agitation and ultrasonic vibration for 10 min. The mixed suspension was evaporated at low pressure under agitation, and dried at 110°C overnight. The composition of the mechanical mixture is expressed as weight ratio R_m with $R_m = 1$ and 0.0 for pure $Fe_2(MoO_4)_3$ and pure α-Sb_2O_4, respectively. Mixtures with $R_m = 0.25$, 0.5 and 0.75 were prepared.

The theoretical bulk atomic ratio were calculated from the bulk weight composition as given by the following equation:

$$R_m = \left(W_{Fe_2(MoO_4)_3}\right) / \left(W_{Fe_2(MoO_4)_3} + W_{\alpha\text{-}Sb_2O_4}\right) \quad (1)$$

2.2. Catalytic activity

2.2.1. Reaction test

The selective oxidation of isobutene to methacrolein was carried out in a conventional fixed bed reactor at atmospheric pressure. Gases were from L'Air Liquide: isobutene 99.0%, O_2 99.95% and N_2 99.8%. The reactor consisted of a Pyrex U-tube of 8 mm internal diameter into which the catalyst was packed. A small tube (4 mm external diameter) for insulating a thermocouple was introduced inside the catalytic bed. The pure oxides or mixtures were pressed, then slightly fragmented and sieved between 500 and 800 μm. The pure oxides ($Fe_2(MoO_4)_3$ and α-Sb_2O_4) were treated exactly in the same way as the mixtures. The catalytic reaction conditions were as follows: the molar ratios in the gas feed were: i-$C_4H_8/O_2/N_2 = 1/2/7$, partial pressure of i-C_4H_8: 76 mm Hg, partial pressure of O_2: 152 mm Hg, total pressure 760 mm Hg, total gas flow (i-$C_4H_8 + O_2 + N_2$): 36 ml min^{-1}; catalyst weight: 300 mg; temperature: 380°C, 400°C, 420°C and 440°C. For each run, the catalyst was heated under the flow of the reaction mixture ($N_2 + O_2$ + isobutene) to the desired temperature. Each run was made with a fresh catalyst. Duration of each test was about 6 h.

2.2.2. Analysis of the reactants and products

The reaction products and the remaining reactants were analyzed by chromatography (Intersmat) employing two columns: Tenax for analyzing the methacrolein and the other oxygenated products and the other one, Porapak Q, for isobutene, CO_2 and water. Taking into account the calibration of the chromatograph equipment, an accuracy of about 2%–3% in the conversion and the yield was obtained.

2.2.3. Expression of the catalytic activity

After reaching the reaction conditions, the catalytic activity was stable in time. No activation nor deactivation phenomenon was observed during the reaction. The reported results correspond to measurements made 1 h after reaching the reaction temperature. As methacrolein is the main selective product (about 95% of the selective oxidation products), only the corresponding results will be reported.

Catalytic activity was expressed as molar yield (Y, %), namely the number of moles of methacrolein produced per moles of isobutene in the feed, the conversion (C, %) as the total fraction of isobutene transformed. The selectivity (S, %) of the reaction was calculated as Y/C.

2.2.4. Synergetic effect on the yield

Pure α-Sb_2O_4 is inactive. The magnitude of the catalytic synergy corresponds to the difference between the yield actually measured with the mixture and that which would be obtained using the amount of $Fe_2(MoO_4)_3$ contained alone. This is given by the following formula:

$$\text{Synergy} = \frac{\left(Y_m - R_m Y_{Fe_2(MoO_4)_3}\right)}{\left(R_m Y_{Fe_2(MoO_4)_3}\right)} \quad (2)$$

where Y_m and $Y_{Fe_2(MoO_4)_3}$ represent the methacrolein yield of, respectively, the mechanical mixture and pure $Fe_2(MoO_4)_3$ measured under the same reaction conditions.

2.3. Physico-chemical characterization

Fresh and used samples were characterized by the following physico-chemical techniques.

2.3.1. BET surface area measurement

Surface area was determined gravimetrically with a Setaram MTB 10-8 microbalance connected to a vacuum and gas handling system. Nitrogen adsorption at -196°C was used.

2.3.2. X-ray diffraction

A Siemens Kristalloflex D-500 diffractometer, using nickel-filtered CuKα radiation was used ($\lambda = 1.54051$ Å, 45 kV and 45 mÅ). Step scan = 1°/min. External calibration with silicon. Siemens goniometer. Crystalline phases were identified by comparison with JCPS data bank of Software DIFRACT-AT/SOCABIM.

2.3.3. Electron microscopy

Electron microscopy examinations were carried out with a Jeol Temscan 100 CX electron microscope equipped with a Kevex 5100 C energy-dispersive spectrometer. The samples were de-aggregated by grinding, dispersed in water and deposited on a carbon film supported on a copper grid and were examined in the CTEM mode.

2.3.4. XPS

As a trade-off between sensitivity and resolution, XPS measurements were carried out in the present investigation in a Vacuum Generator ESCA-3 MK II equipment. The exciting radiation was Mg Kα (1253.6 eV). The analyser energy was 50 eV. In this case, the Full Width at Half Maximum (FWHM) of $Au4_{f7}$ was about 2 eV. As no flood-gun was equipped in this machine, the resolution was lower with insulating substances such as α-Sb_2O_4 (the FWHM of $Sb3p_{3/2}$ is about 2.5 eV). The binding energy of the concerned elements was calculated taking the carbon peak C1s (284.6 eV) as a reference. The surface concentrations were calculated from

the normalised XPS intensities using the sensitivity factors given by Wagner et al. [22]. For Sb, the $Sb3d_{3/2}$ line was used instead of $Sb3d_{5/2}$, because of the superposition of the $Sb3d_{5/2}$ and O1s peaks. Mo3d and Fe2p3 were used for calculating the concentration of Mo and Fe, respectively. The Fe/Mo, Sb/(Fe + Mo + Sb) and Mo/(Fe + Mo + Sb) XPS atomic ratios were calculated.

2.3.5. ISS

The instrument was a Kratos spectrometer (Wg 541–515), which has been described in detail elsewhere [4,23]. A mixture of He and Xe ions with an energy of 2 keV was used to raster a square area (1.5×1.5 mm^2) of the sample. The ion currents for He and Xe were about 10 and 5 nA, respectively. The ISS signals only come from He^+; Xe being used just for sputtering (progressive surface erosion). As the sputtering rate with He is extremely low, only the ion dose (or fluence) of Xe will be taken into account for the depth profiling measurements. The ion dose was calculated by $F = I_0 \times t/1.6 \times 10^{-19}$, with F in ions/cm^2, I_0 in A/cm^2, and t the time of bombardment in seconds. In our measurements, each spectrum accumulated 100 scans recorded during a total time of 400 s. This corresponds to an ion dose of 0.5×10^{15} Xe ions/cm^2. According to literature, the sputtering yield for Mo and Fe with Xe (2 keV) is 1–2 [24]. No sputtering yield with Xe was mentioned for Sb. It can be assumed [25] that the sputtering yields for oxides are similar to those of the corresponding metals. If we assume that the sputtering yields for Fe, Mo in $Fe_2(MoO_4)_3$ and Sb in α-Sb_2O_4 are in the range of 1 to 2 and taking into account the surface atomic density of the oxides (e.g., 1.67×10^{15} atoms/cm^2 for α-Sb_2O_4 [4]), it can be approximately estimated that an ion dose of about $1–2 \times 10^{15}$ Xe ions/cm^2 is required to remove one monolayer.

2.3.6. Mössbauer spectroscopy

The Fe Mössbauer spectra were recorded with a constant velocity spectrometer connected to a Northern NS-900 multichannel analyser, using a

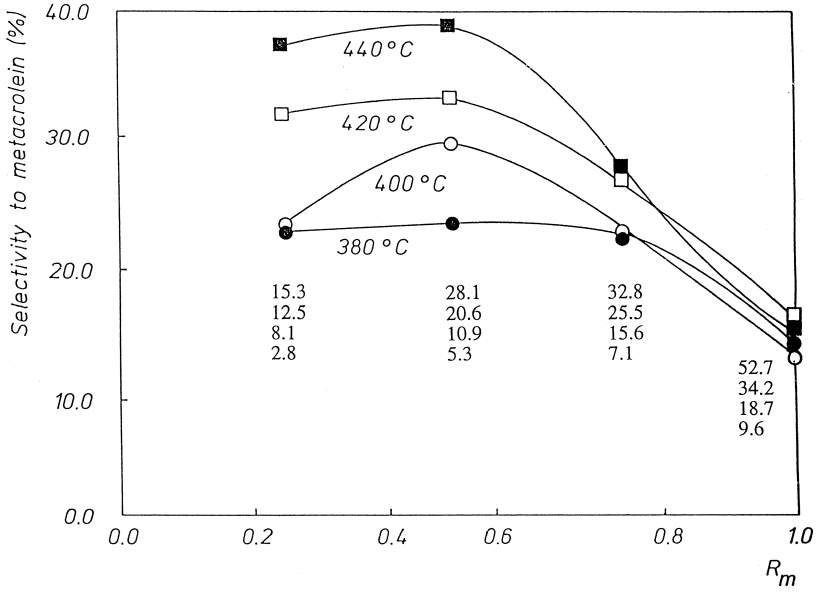

Fig. 1. Effect of composition (R_m) of the mechanical mixtures on selectivity to methacrolein (iso-$C_4H_8/O_2/N_2 = 1/2/7$). Conversions in % in order of decreasing temperature are indicated below the experimental points corresponding to each R_m.

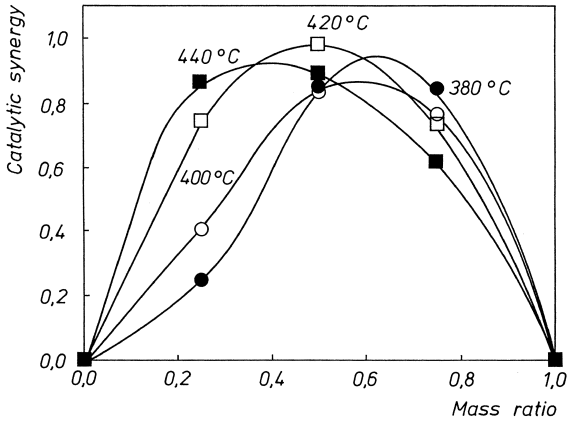

Fig. 2. Synergy on the yield (calculated from Eq. (2)) as a function of composition (R_m).

10-mCi ^{57}Co/Rh source. The Mössbauer parameters were estimated by a least sequence computer fit. Isomer shift (IS) was calculated with reference to α-Fe. Experimental error for IS was ± 0.05 mm/s.

3. Results

3.1. Catalytic test

3.1.1. Catalytic test under standard conditions

α-Sb_2O_4 is inert. The conversion increases, in an approximately linear way, as the amount of $Fe_2(MoO_4)_3$ in the mechanical mixtures increases for all temperatures investigated. Selectivity markedly increases when $Fe_2(MoO_4)_3$ is mixed with α-Sb_2O_4 and increases when temperature increases (Fig. 1). The variation of synergy, as defined by Eq. (2), vs. composition is represented in Fig. 2. The additional production of methacrolein due to the presence of α-Sb_2O_4 is between 20% and 95%, depending of the temperature and the amount of α-Sb_2O_4, namely 20% to 95% of the one which would be obtained with pure $Fe_2(MoO_4)_3$, if it kept the same activity as when pure. When the reaction temperature increases, the composition (R_m) at

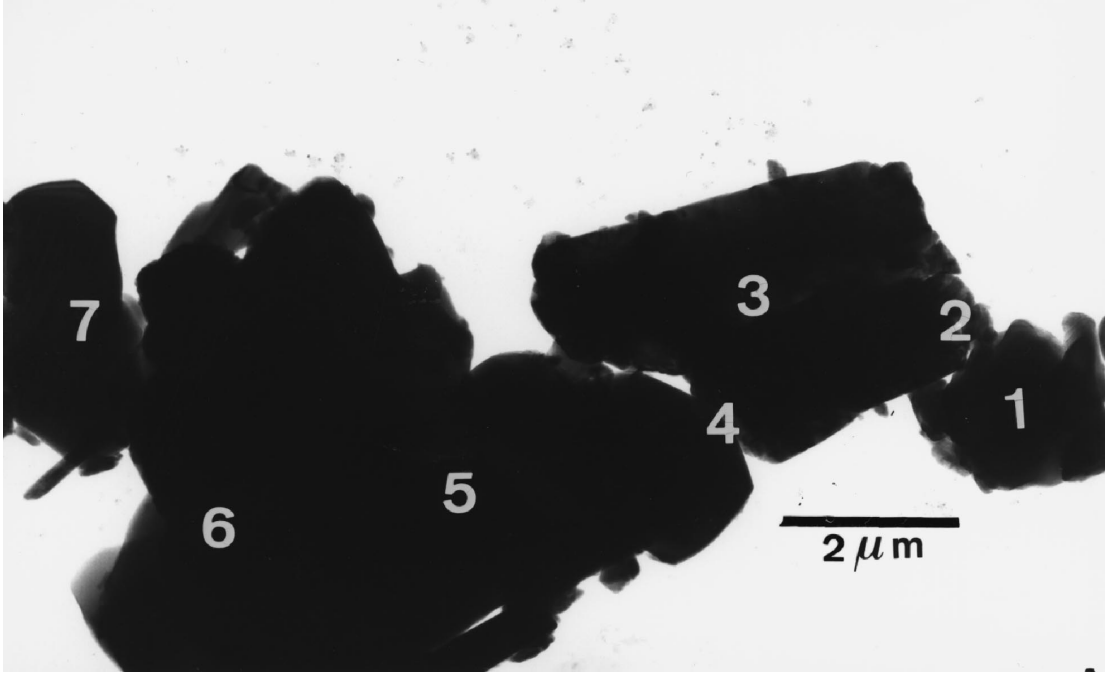

Fig. 3. Typical CTEM micrograph of used $Fe_2(MoO_4)_3$ + α-Sb_2O_4 mechanical mixtures with $R_m = 0.5$.

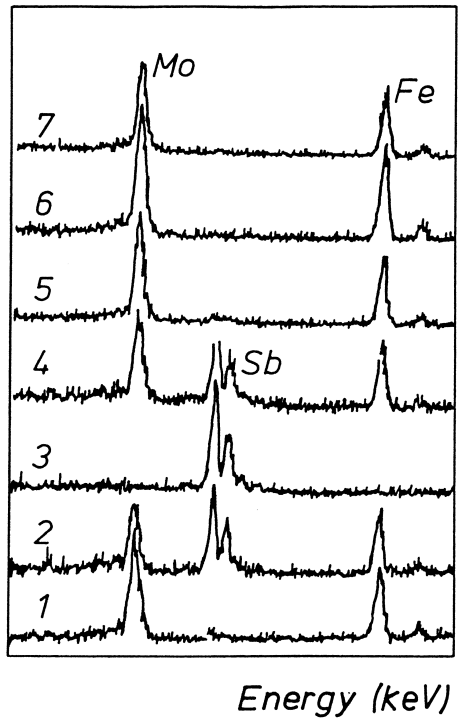

Fig. 4. Electron Probe Microscopy Analysis of used $Fe_2(MoO_4)_3$ + α-Sb_2O_4 mechanical mixture with $R_m = 0.5$.

which the maximum synergy is observed decreases.

3.2. Characterization

3.2.1. BET analysis and XRD

The BET surface area of the mechanical mixture is the simple sum of those of the pure oxides. No detectable change in the BET surface area occurs during reaction either for pure oxides or for mechanical mixtures.

The XRD diffraction lines of mechanical mixtures, fresh or used in the standard catalytic test, correspond to the simple superposition of those observed in pure $Fe_2(MoO_4)_3$ and α-Sb_2O_4. No new phases were observed.

3.2.2. CTEM and EPMA analysis

Fig. 3 shows a typical micrograph obtained with a used mechanical mixture corresponding to $R_m = 0.5$. Identical pictures were obtained with fresh mixtures. The particle or aggregate size of $Fe_2(MoO_4)_3$ is comparable to that of α-Sb_2O_4 (about 5 μm). Morphologically, no difference is observed between α-Sb_2O_4 and $Fe_2(MoO_4)_3$. EPMA was also carried out for fresh and used samples at different locations. Using a representative sample of used catalysts, these locations are shown in CTEM micrography (numbers 1–7) in Fig. 4. Some particles correspond to pure iron molybdate. One particle corresponds to α-Sb_2O_4. Some aggregates associate particles of both species, that the relatively low resolution of EPMA (about 1 μm) cannot distinguish. Even for used samples, only the Sb, or both the Fe and Mo signals, are detected when the analysis is made on, respectively, the α-Sb_2O_4 particle or on $Fe_2(MoO_4)_3$ particles.

3.2.3. XPS analysis

Table 1 summarizes the binding energies of the XPS peaks for pure oxides and mechanical mixtures. The binding energy at 540.0 eV is attributed to $Sb3d_{3/2}$ electrons in α-Sb_2O_4 and

Table 1
XPS binding energy values in (eV) for pure $Fe_2(MoO_4)_3$ and $Fe_2(MoO_4)_3$–α-Sb_2O_4 mechanical mixtures

Sample	Fresh sample			Used sample		
	$Mo3d_{5/2}$	$Fe2p_{3/2}$	$Sb3d_{3/2}$	$Mo3d_{5/2}$	$Fe2p_{3/2}$	$Sb3d_{3/2}$
$Fe_2(MoO_4)_3$	232.5	711.9		232.6	711.9	
MM ($R_m = 0.75$)	232.8	711.7	540.1	232.7	711.9	540.1
MM ($R_m = 0.50$)	232.6	711.8	540.0	232.6	711.8	540.1
MM ($R_m = 0.25$)	232.7	711.6	539.9	232.7	711.8	540.1
α-Sb_20_4			540.0			540.0

that at about 232.7 eV to $Mo3d_{5/2}$ electrons in $Fe_2(MoO_4)_3$. Binding energies are identical (to about 0.2 eV) in the mixtures and in the pure oxides. They remain unchanged after catalytic test. Comparison of the FWHM of Sb3d3 for each mechanical mixture before and after reaction shows no change. The XPS Fe/Mo atomic ratio is nearly identical for all the fresh samples (at about 0.290). After reaction, this ratio is identical for all compositions but slightly lower than that of the fresh ones (0.270). The XPS Sb/(Fe + Mo + Sb) and Mo/(Fe + Mo + Sb) atomic ratios vary linearly with the bulk (Mo + Fe)/Mo + Fe + Sb) atomic ratio (Fig. 5). Comparing the values observed before and after test, they remain (with a precision of about 10%) practically unchanged.

3.2.4. ISS measurement

Pure $Fe_2(MoO_4)_3$ and α-Sb_2O_4 and the mechanical mixture of composition $R_m = 0.5$ were investigated. Fig. 6 presents the ISS intensities of Mo and Sb as a function of the Xe ion dose (fluence) for the mechanical mixture of $Fe_2(MoO_4)_3$ and α-Sb_2O_4 with $R_m = 0.5$, before and after reaction. The intensity of the Fe was not presented because of the low value of the corresponding signal. It can be observed that the ISS intensities of both Mo and Sb increase progressively with Xe ions dose and reach a plateau when the Xe ions dose is greater than about 1.5×10^{15} ions/cm^2. The intensities of Mo and Sb in the mechanical mixtures at the plateau are the half of those obtained with pure $Fe_2(MoO_4)_3$ and α-Sb_2O_4. In other words, the spectrum of the mechanical mixture is exactly the sum of those of pure oxides divided by two. For the mechanical mixture after reaction, the intensities of both Mo and Sb are the same as those obtained with the fresh sample. Concerning Fe, the signal (of low intensity) is very similar in pure $Fe_2(MoO_4)_3$ and in the mechanical mixture and is identical, before and after reaction.

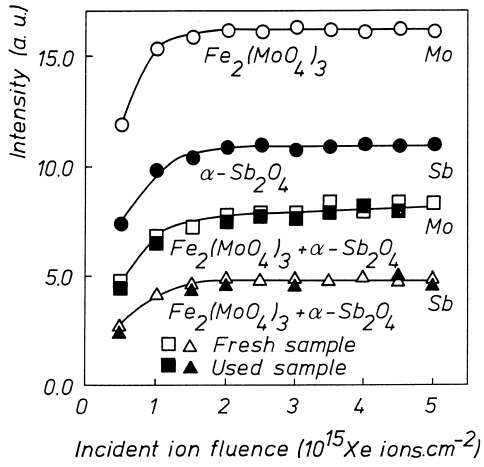

Fig. 6. ISS intensities of Mo, and Sb as a function of Xe ion dose for pure α-Sb_2O_4, pure $Fe_2(MoO_4)_3$ and $Fe_2(MoO_4)_3 + \alpha$-Sb_2O_4 mechanical mixture with $R_m = 0.5$. Before and after reaction.

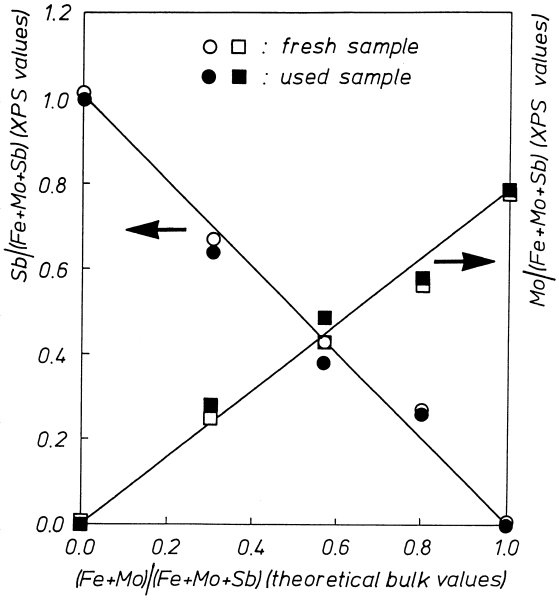

Fig. 5. XPS results. Sb/(Fe + Mo + Sb) and Mo/(Fe + Mo + Sb) XPS surface relative atomic ratio as a function of the theoretical bulk (Mo + Fe)/(Fe + Mo + Sb) atomic ratio for mechanical mixtures of $Fe_2(MoO_4)_3 + \alpha$-Sb_2O_4. Black symbol: fresh sample. Open symbol: used sample.

3.2.5. Mössbauer spectroscopy

The Mössbauer spectroscopy measurements were made on a mixture with $R_m = 0.5$ (Fig. 7). It is observed that the spectrum is exactly the same as that of pure $Fe_2(MoO_4)_3$. The IS (δ) at room temperature is 0.40 min s^{-1} and the

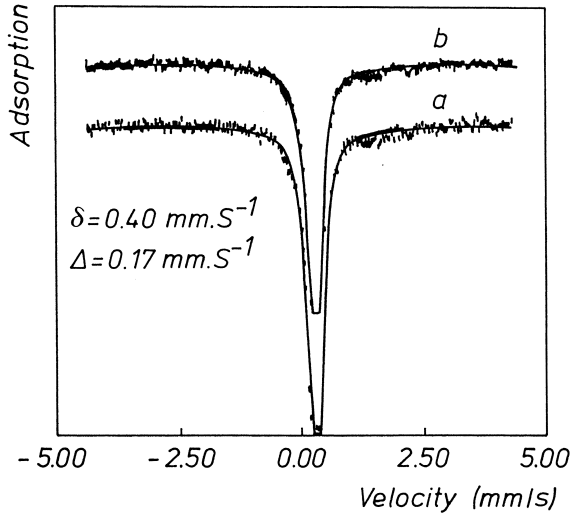

Fig. 7. Room temperature Mössbauer spectra of the fresh (a) and used (b) $Fe_2(MoO_4)_3$–α-Sb_2O_4 mechanical mixture with R_m = 0.5.

quadrupole splitting (Δ) is 0.17 min s^{-1}. No change is observed between fresh and used samples.

4. Discussion

We shall first discuss the results of physicochemical characterization in view of examining the possible occurrence of contamination. A second section will discuss the synergetic effects.

4.1. Existence of possible interaction between $Fe_2(MoO_4)_3$ and α-Sb_2O_4

4.1.1. Possible formation of new phases

XRD does not detect any new phases. Only phases corresponding to pure $Fe_2(MoO_4)_3$ and α-Sb_2O_4 were observed. Mössbauer spectroscopy shows that the IS (δ) and quadrupole splitting (Δ) of Fe in the mechanical mixture before and after reaction are the same as those observed with pure $Fe_2(MoO_4)_3$. These two techniques show that no new phase (even an amorphous phase, Mössbauer results), was formed either during the preparation of the mechanical mixture or after the catalytic reaction under our reaction conditions. This conclusion is in agreement with the finding of Cadus et al. [10] that a temperature of 500°C (60°C higher than the highest temperature we used) applied at least for 2 days in air is necessary to initiate the formation of $FeSbO_4$. On the other hand, a phase associating Mo and Sb is still more difficult to form [2,26,27]. However, as these two techniques are bulk techniques, the formation of a very small amount of some new phases beyond the detection limit of these two techniques (lower than 2%–3%) cannot be absolutely excluded.

4.1.2. Existence of some possible surface contamination

Let us thus examine carefully the possibility of $FeSbO_4$ formation. Important is to underline that the surface area of the mixtures remains unchanged after the reaction. This strongly suggests that, if a layer of a new phase (which should probably be $FeSbO_4$) is formed, the size of the crystallites of this layer would have about the same size as the pure oxides forming the mixture. If smaller, an increase of the surface area should be observed. The only hypothesis to examine is therefore the formation of a uniform layer of $FeSbO_4$. The corresponding reaction implies the transfer of Fe from $Fe_2(MoO_4)_3$ to α-Sb_2O_4. Let us assume that a layer of about 10 Å of $FeSbO_4$ is actually formed on the surface of α-Sb_2O_4. If we consider that the surface of the (100) face of a unit cell of $FeSbO_4$ is the same as that of α-Sb_2O_4 (namely 0.16 nm^2), and taking into account that the surface area of both oxides is about 2.5 m^2 g^{-1}, the calculated amount of the formed layer would correspond to about 1.5 wt.% of the oxides forming the mixture. This low amount obviously cannot be detected by XRD. Taken into account the fact that the analysis depth of XPS for Sb is about $3\lambda_{Sb3d3} \times \cos\theta$, where λ_{Sb3d3} is the inelastic mean free path of the electrons Sb3d3 (λ_{Sb3d3} = 12 Å [5]), and θ is the take-off angle of analysis (in our case $\theta = 45°$), the contribution of this

layer in the total integrated XPS intensity of Sb3d3 would be about 58%. This indicates that the Sb3d3 peak should be composed of two parts, one with a binding energy of 540.1 eV (about 42%) and the other with a binding energy of 540.6 eV (about 58%). The measured binding energy would be $540.1 \times 0.42 + 540.6 \times 0.58 = 540.34$ eV, which is 0.2 eV higher than the measured value of α-Sb_2O_4. Taking into account the FWHM of Sb3d3 in α-Sb_2O_4 and $FeSbO_4$ (2.5 eV), the FWHM of the Sb3d3 peak (always assuming a layer of 10 Å on α-Sb_2O_4) can be estimated by simulation as 2.57 eV, which is 0.07 eV higher than in α-Sb_2O_4. The above calculation suggests that the presence of $FeSbO_4$ cannot be detected when its layer is of the order of 10 Å. Therefore, we are obliged to concluded that XPS cannot give informations more precise than XRD (complemented by Mössbauer spectroscopy) when the depth of a hypothetical layer of $FeSbO_4$ is about or lower than 10 Å.

With respect to the more surface-sensitive technique, ISS, if such a layer (10 Å) of $FeSbO_4$ was formed on the surface of α-Sb_2O_4, some modification in the intensity should be expected. More precisely, the surface concentration and the ISS signal of Fe should increase in the case of the mechanical mixture after reaction. If the crystallites of the new formed layer were cubics (surface of (100) face = 0.16 nm^2 and high = 0.4 nm^2), and if no agglomeration of particles occurred, this layer of 10 Å would correspond to the formation of 2.5 monolayers of $FeSbO_4$ on the surface of α-Sb_2O_4. During the formation of the layer, half of the surface of α-Sb_2O_4 would be contaminated by Fe ions. As with an ion fluence of $1–2 \times 10^{15}$ Xe ions/cm^2, one layer of the surface is removed, then the ISS signal of Fe should increase by 50% at least during the erosion of the first two layers of the $FeSbO_4$ formed. This high value of the Fe signal has to remain during the erosion of 2.5 layers (about 4×10^{15} Xe ions/cm^2). This has not been observed in our results. In conclusion, as the investigation using ISS fails to detect the presence of $FeSbO_4$, we must conclude that its presence (if any) is under the detection limit of all techniques we used.

Table 2 shows that the binding energy of Fe2p3 remains constant before and after reaction under standard conditions. Taking into account the fact that the binding energy of Fe^{+2} is about 1 eV lower than that of Fe^{+3} [28], this result shows that the reduction of $Fe_2(MoO_4)_3$ (in $FeMoO_4$) is lower than the detection limit of XPS.

Other indications concerning this problem could come from the signals of the other elements. The particle size of both oxides is similar and does not change either after mixing or after catalytic reaction, as evidenced by our electron microscopy results. Therefore, if there is no surface contamination, the surface concentration should be proportional to the bulk one. This is exactly what we observe in Figs. 5 and 6. In Fig. 6, the ISS intensity of both Mo and Sb in mechanical mixtures varies exactly in the same manner as in pure $Fe_2(MoO_4)_3$ and α-Sb_2O_4 oxides. The surface composition is the same as in the bulk. The initial rise of ISS intensity is commonly observed and can be explained by the desorption of adsorbed molecules, e.g., hydrocarbons, oxygen and water, upon bombardment [23]. The initial rise corresponds approximately to the removal of about 1 monolayer. One remark from Fig. 5 is that the Mo/(Mo + Fe + Sb) ratios calculated from XPS results are higher than the theoretical bulk ones (e.g., about 0.78 for pure $Fe_2(MoO_4)_3$ instead of 0.60). This effect is associated with the very low Fe/Mo ratio (0.29 compared to the theoretical value 0.67) determined by XPS for pure $Fe_2(MoO_4)_3$. This low Fe/Mo value may suggest some Mo enrichment on the $Fe_2(MoO_4)_3$ surface. However, this suggestion is not confirmed by ISS results because, if Mo was enriched at the surface, the ISS intensity of Mo should decrease with the ion bombardment, which is not observed in Fig. 6. We believe that the low Fe/Mo value observed by XPS may be explained by two possibilities: (1) the use of not

adequate sensitivity factors in this work, particularly for Fe2p3 [29] and (2) the difficulty of choosing the baseline for Fe2p3 due to the presence of an Auger peak of oxygen in close proximity.

The above discussions allow us to conclude that within the detection limit of our techniques, the mechanical mixtures of $Fe_2(MoO_4)_3$ and α-Sb_2O_4 are composed of two pure, uncontaminated phases. This is true for fresh and used samples.

4.2. Synergy between α-Sb_2O_4 and $Fe_2(MoO_4)_3$

Account taken of the narrow similitude of the present effects with those observed with many other mixtures of powders [1–14], the most probable explanation for the synergism observed in our experiments is the existence of a RCM. An additional reason suggesting this conclusion is that α-Sb_2O_4 has been found in very many cases to increase selectivity and activity of other phases (e.g., MoO_3, pure SnO_2 or Sb saturated SnO_2, $ZnFe_2O_4$, ...). As in these cases, α-Sb_2O_4 controls the catalytic activity of $Fe_2(MoO_4)_3$ via the spillover oxygen it produces. This spillover oxygen flows on $Fe_2(MoO_4)_3$ and keeps it in a more selective and active state. It must however be emphasized that this conclusion holds only for the relatively short duration of the experiments reported here (about 6 h). From the account taken from experiments of longer duration [10], it seems that this is due to the length of the induction time in the nucleation of $FeSbO_4$ (about 2 days at temperatures higher than those used here).

The conversion increases, in an approximately linear way, as the amount of $Fe_2(MoO_4)_3$ in the mechanical mixtures increases. There is nothing surprising in that. The important fact is that the methacrolein yield and the selectivities obtained with the mechanical mixtures are higher than those of the pure $Fe_2(MoO_4)_3$ (Figs. 1 and 2). When R_m decreases from 0.5 to 0.25, the conversion decreases in the same proportion but the selectivity remains constant (Fig. 1). The higher selectivity with mechanical mixtures, therefore, cannot be attributed to a purely kinetic effect, namely the lower conversion with smaller R_m, which would supposedly diminish the degradation of methacrolein. The addition of α-Sb_2O_4 enhances principally selectivity. This is a characteristic feature of the remote control effect. The role of spillover oxygen is to maintain (or to restore) selectivity of the catalytic sites on $Fe_2(MoO_4)_3$. The approximate linearity in conversion indicated above shows that the number of isobutene molecules converted in a given time on a given weight of $Fe_2(MoO_4)_3$ is constant. Assuming an identical turnover frequency, this would imply that the total number of active sites, selective or not, remains the same whether the remote control operates or not. The difference is that the active sites become more selective in the mechanical mixtures. In fact, 233 mg (300×0.75) of $Fe_2(MoO_4)_3$ when mixed with α-Sb_2O_4 (inactive) produces 20% more methacrolein than 300 mg of pure $Fe_2(MoO_4)_3$ (yield of 9.2% and 7.6%, respectively).

The plot of Fig. 1 suggests that α-Sb_2O_4 supplies sufficient spillover oxygen to $Fe_2(MoO_4)_3$ as long as it represents about 50% by weight of the mixture. For lower proportions (higher R_m), $Fe_2(MoO_4)_3$ is not sufficiently irrigated and the selectivity drops. The selectivity of the sites on $Fe_2(MoO_4)_3$ thus seems to necessitate that the surface be in a high oxidation state. Catalytic activity measurements involving changes of the oxygen to isobutene ratio (O_2/i-C_4H_8), in particular using low oxygen partial pressure, were realized in another work [30]. Experiments were made with catalysts of composition $R_m = 0.5$ and $R_m = 1.0$ (namely pure $Fe_2(MoO_4)_3$). The results showed that at high O_2/i-C_4H_8, the isobutene conversion was almost six times higher for pure $Fe_2(MoO_4)_3$ than for the mechanical mixture. When the O_2/i-C_4H_8 increased, the selectivity to methacrolein decreased, significantly for pure $Fe_2(Mo_4)_3$ but the selectivity with the mechani-

cal mixture remained always higher than that with pure $Fe_2(MoO_4)_3$. For a $O_2/i\text{-}C_4H_8$ molar ratio equal to one, pure $Fe_2(MoO_4)_3$ was reduced to $FeMoO_4$, while no reduction was observed in the $Fe_2(MoO_4)_3 + \alpha\text{-}Sb_2O_4$ mechanical mixture. When the $O_2/i\text{-}C_4H_8$ molar ratio was lower, both samples were reduced, but pure $Fe_2(MoO_4)_3$ got more reduced, as indicated by the formation of a detectable quantity of segregated MoO_{3-x}.

These results show that the pure acceptor ($Fe_2(MoO_4)_3$) behaves differently from mechanical mixtures when the partial pressure of oxygen is changed, supporting the conclusion that spillover oxygen creates selective sites during the catalytic reaction in the present case, mainly by avoiding the formation of reduced phases and this because it maintains the catalytic sites in a higher oxidation state.

Thanks to the present results, we can demonstrate that a synergy exists between fresh $\alpha\text{-}Sb_2O_4$ and $Fe_2(MoO_4)_3$, before any substantial solid state reaction takes place in the mixture. $Fe_2(MoO_4)_3$ had been considered by many investigators to represent a catalyst by itself. Although we cannot exclude that other mechanism different from the RCM could operate simultaneously after solid state reactions have taken place, the present work shows that $Fe_2(MoO_4)_3$ needs to be accompanied by a donor phase to achieve better performances. It is known that the ''iron molybdate'' catalysts used for the oxidative dehydrogenation of methanol to formaldehyde always contain a large excess of MoO_3 beside $Fe_2(MoO_4)_3$. We have shown that MoO_3 in that case is the main active phase. It is kept active by a spillover donor ($\alpha\text{-}Sb_2O_4$) [31]. We may speculate that $Fe_2(MoO_4)_3$ and/or $FeMoO_4$ in the case of ''iron molybdate'' actually plays a role of donor [31]. These results fit in the frame of the picture that the remote control theory offers for multicomponent catalysts.

This work shows that $\alpha\text{-}Sb_2O_4$ as a donor is important to improve the catalytic performances of $Fe_2(MoO_4)_3$. But this is not an exclusive property of $\alpha\text{-}Sb_2O_4$. As we have previously discussed, other oxides can be better donors than $\alpha\text{-}Sb_2O_4$ and the corresponding synergetic effect could possibly be significantly increased. We have proposed a scale of acceptor–donor properties of oxides often used in selective oxidation catalysts [1,2]. This scale can be useful to select the most adequate donor and optimize cooperative effects via the RCM. It is not impossible that supports used or tentatively used in selective oxidation catalysts might play a similar role. Although we have not yet gathered information in this respect, SiC or high temperature resistant oxides might perhaps be investigated in this context.

5. Conclusions

A synergy exists between $\alpha\text{-}Sb_2O_4$ and $Fe_2(MoO_4)_3$ in the oxidation of isobutene to methacrolein, although other mechanisms may explain the activity after long reaction times.

Investigations using BET surface area, CTEM, EPMA, XRD, Mössbauer spectroscopy, XPS and ISS fail to detect any mutual contamination after the $\alpha\text{-}Sb_2O_4 + Fe_2(MoO_4)_3$ mechanical mixtures have worked catalytically for about 6 h.

It is proposed that the synergy is due to a remote control, namely that $\alpha\text{-}Sb_2O_4$ (inactive in the oxidation reaction) emits spillover oxygen which maintains the active centers on $Fe_2(MoO_4)_3$ selective.

This effect is due to the ability of spillover oxygen to maintain the surface of $Fe_2(MoO_4)_3$ in a highly oxidised state.

Acknowledgements

The ‘Service de Programmation de la Politique Scientifique, Belgium’ is gratefully acknowledged for its Concerted Action grant to the laboratory CATA, especially for the support of Dr. P. Ruiz. The XPS and the ISS equip-

ments were acquired thanks to a grant from the Fonds National pour la Recherche Scientifique of Belgium. The stay in Belgium of Y.L. Xiong took place in the frame of a cooperation agreement with China supported by the European Community, which is gratefully acknowledged. We are indebted to Dr. J. Naud for his help in XRD measurements, Mr. C. Poleunis for ISS measurements and to Mr. M. Genet for his constructive discussions and comments concerning the XPS analyses.

References

[1] L.T Weng, P. Ruiz, B. Delmon, in: P. Ruiz, B. Delmon (Eds.), Studies in Surface Science and Catalysis, New Developments in Selective Oxidation by Heterogeneous Catalysis, Vol. 72, Elsevier, 1992, pp. 399–413.
[2] L.T. Weng, B. Delmon, Appl. Catal. A 81 (1992) 141.
[3] B. Zhou, E. Sham, T. Machej, P. Bertrand, P. Ruiz, B. Delmon, J. Catal. 132 (1991) 157.
[4] B. Zhou, T. Machej, P. Ruiz, B. Delmon, J. Catal. 132 (1991) 183.
[5] L.T. Weng, N. Spitaels, B. Yasse, J. Ladrière, P. Ruiz, B. Delmon, J. Catal. 132 (1991) 319.
[6] L.T. Weng, B. Yasse, J. Ladrière, P. Ruiz, B. Delmon, J. Catal. 132 (1991) 343.
[7] L.T. Weng, Y.L. Xiong, P. Ruiz, B. Delmon, Tokyo Conference Catal. Sci. Technol., Tokyo, 1990, Catalytic Science and Technology 1 (207) (1991) Kodansha, Japan.
[8] C. Li, Q. Xin, Z.X. Guo, P. Ruiz, B. Delmon, J. Mol. Catal. 72 (1992) 30.
[9] P. Ruiz, Ph. Bastians, L. Caussin, R. Reuse, L. Daza, D. Acosta, B. Delmon, Catal. Today 16 (1993) 99.
[10] L.E. Cadus, F.J. Gotor, D. Acosta, J. Naud, P. Ruiz, B. Delmon, Solid State Ionics 63–65 (1993) 743.
[11] R. Castillo, P.A. Awasarkar, Ch. Papadopoulou, D. Acosta, P. Ruiz, B. Delmon, Studies in surface science and catalysis, in: V. Cortés Corberán, S. Vic Bellón (Eds.), New Development in Selective Oxidation II, 82, 1994, p. 795.
[12] L.E. Cadus, Y.L. Xiong, F.J. Gotor, D. Acosta, J. Naud, P. Ruiz, B. Delmon, Studies in surface science and catalysis, in: V. Cortés Corberán, S. Vic Bellón (Eds.), New Developments in Selective Oxidation II, 82, 1994, p. 41.
[13] B. Delmon, P. Ruiz, S.R.G. Carrazan, S. Korili, M.A. Vicente Rodriguez, Z. Sobalik, 2nd Conference on Catalyst in Petroleum Refining, Safat, Kuwait, 19–22, April, 1995, in: M. Absi-Halabi, J. Beshara, H. Qabazard, A. Stanislas (Eds.), Catalysis in Petroleum Refining and Petrochemical Industries, Elsevier, Amsterdam, The Netherlands, 1996, pp. 1–25.
[14] F.Y. Qiu, L.T. Weng, E. Sham, P. Ruiz, B. Delmon, Appl. Catal. 51 (1989) 235.
[15] G. Mestl, P. Ruiz, B. Delmon, H. Knözinger, J. Phys. Chem. 98 (1994) 11283.
[16] L.T. Weng, P. Ruiz, B. Delmon, D. Duprez, J. Mol. Catal. 52 (1989) 349.
[17] D. Martin, P. Kaur, D. Duprez, E. Gaigneaux, P. Ruiz, B. Delmon, Catal. Today 32 (1996) 326.
[18] E. Gaigneaux, P. Tsiakaras, D. Herla, L. Ghenne, P. Ruiz, B. Delmon, American Chemical Society Annual Meeting, Symposium on ''Catalysis and Photocatalysis on Metal Oxides'', ACS Book Division, Chicago, August 21–25, 1995.
[19] S.R.G. Carrazan, C. Peres, J.P. Bernard, P. Ruiz, B. Delmon, J. Catal. 158 (1996) 452.
[20] S.A. Korili, P. Ruiz, B. Delmon, Catal. Today 32 (1996) 229.
[21] A. Gil, P. Ruiz, B. Delmon, Catal. Today 32 (1996) 329.
[22] C.D. Wagner, L.E. Davis, M.V. Zeller, J.A. Teller, R.H. Raymond, L.H. Gale, Surf. Interface Anal. 3 (1981) 211.
[23] P. Bertrand, J.M. Beuken, M. Delvaux, Nucl. Instrum. Methods Phys. Res. 218 (1983) 249.
[24] H.H. Andersen, H.L. Bay, in: R. Behrisc (Ed.), Sputtering by Particles Bombardment I, Topics in Appl. Phys., Vol. 52, Springer-Verlag, Berlin, 1983, p. 57.
[25] G. Bertz, G.K. Wehner, in: R. Behrisc (Ed.), Sputtering by Particles Bombardment II, Topics in Appl. Phys., Vol. 47, Springer-Verlag, Berlin, 1981, p. 145.
[26] N. Burriesci, F. Garbassi, M. Petrera, G. Peterini, J. Chem. Soc., Faraday. Trans. 1 78 (1982) 817.
[27] M. Carbucicchio, G. Centi, F. Trifiro, J. Catal. 91 (1985) 85.
[28] D. Briggs, M.P. Seah, Practical Surface Analysis, 2nd edn., Vol. 1, Wiley, Chichester, 1990, p. 607.
[29] L.T. Weng, G. Vereecke, M.J. Genet, P. Rouxhet, J.H. Stone-Masui, P. Bertrand, W.E.E. Stone, Surf. Interface Anal. 20 (1993) 193.
[30] Y.L. Xiong, S. Gonzalez Carrazan, L.E. Cadus, D. Acosta, J. Naud, P. Ruiz, B. Delmon, to be submitted.
[31] R. Castillo, K. Dewaelle, P. Ruiz, B. Delmon, Appl. Catal., A 153 (1997) L1–L8.